arXiv:2507.07138v2 [cs.LG] 4 Nov 2026

GNNs Meet Sequence Models Along the Shortest-Path: an Expressive Method for Link Prediction

Francesco Ferrini[*,1] **Veronica Lachi**[*,2] **Antonio Longa**[2] **Bruno Lepri**[1] **Andrea Passerini**[3]

[1]Fondazione Bruno Kessler, Trento, Italy
[2]The Arctic University of Norway, Tromsø, Norway
[3]University of Trento, Trento, Italy

Abstract

Graph Neural Networks (GNNs) often fail to capture the link-specific structural patterns essential for accurate link prediction, since their node-centric message passing might overlook the subgraph structures connecting two nodes. Prior attempts to inject such structural context either suffer from high computational cost or rely on oversimplified heuristics (e.g., common neighbor counts) that cannot capture multi-hop dependencies. We propose SP4LP (Shortest Path for Link Prediction), a new framework that integrates GNN-based node encodings with sequence modeling over shortest paths. Specifically, SP4LP first computes node representations with a GNN, then extracts the shortest path between each candidate node pair and processes the sequence of node embeddings with a sequence model. This design allows SP4LP to efficiently capture expressive multi-hop relational patterns. Theoretically, we show that SP4LP is strictly more expressive than both standard message-passing GNNs and several leading structural feature methods, positioning it as a general and principled framework for link prediction in graphs. Empirically, SP4LP sets a new state of the art on many standard link prediction benchmarks.

1 Introduction

Graph Neural Networks (GNNs) are widely adopted for link-level tasks such as link prediction [23, 27, 48, 51], link classification [7, 32, 41] and link regression [11, 25] with applications spanning recommender systems [46], knowledge graph completion [31], and biological interaction prediction [18].

Despite their popularity, standard GNNs struggle to accurately represent links, as they typically construct link embeddings by aggregating the representations of the two endpoint nodes. This node-centric strategy leads to a key limitation: structurally distinct links may be mapped to the same representation when their endpoints are automorphic [4, 35, 49]. For example, in the graph of Figure 1, links (v, u) and (v, u') yield identical representations under any standard GNN, even if one pair shares a common neighbor and the other does not. This issue, known as the automorphic node problem [4], highlights a fundamental expressivity bottleneck in message-passing schemes for link representation.

To address this, several methods enhance GNNs with structural features (SFs), which can be broadly classified into three paradigms [42]: SF-then-GNN, which injects structural context into the graph before message passing (e.g., SEAL [49], NBFNet [52]); SF-and-GNN, which computes SFs and node embeddings in parallel (e.g., Neo-GNN [47], BUDDY [4], MPLP [12]); and GNN-then-SF,

*Equal contribution. Corresponding authors: fferrini@fbk.eu, veronica.lachi@uit.no

40th Conference on Neural Information Processing Systems (NeurIPS 2026).

which applies message passing once to compute node representations and then combines them using task-specific structural context (e.g., NCN and NCNC [42]).

While SF-then-GNN methods are expressive, they are computationally inefficient, often requiring subgraph extraction or retraining per link. SF-and-GNN models are efficient but rely on predefined heuristics, limiting their ability to capture rich relational patterns. GNN-then-SF approaches offer a compelling trade-off between expressivity and scalability, but current methods in this class, i.e., NCN and NCNC, still rely on overlap between the neighborhoods of the endpoints: NCN uses common neighbors, while NCNC also leverages predicted second-order common neighbors. In the absence of such overlapping neighbors, they revert to standard GNN behavior and lose expressive power.

In this paper we propose SP4LP, a novel method in the GNN-then-SF paradigm that combines high expressiveness with computational efficiency. SP4LP constructs a path-aware representation by incorporating the embeddings of all nodes along the shortest path connecting the two endpoints. These node embeddings, obtained via a base GNN, are then processed as a sequence using a dedicated sequence model, such as a Transformer [37], LSTM [16], or an injective summation function [43].

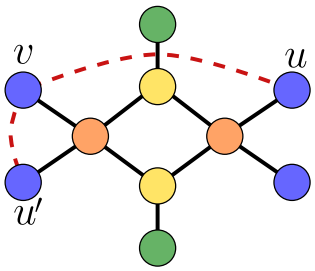

Figure 1: Links (v, u) and (v, u') have different structural roles within the graph, yet a GNN assigns them identical representations.

The first key advantage of SP4LP is its **expressiveness**. Unlike structural features such as common neighbors, which may not exist for many node pairs and can lead to degenerate cases in sparse graphs, the shortest path is always defined between any two nodes if the graph is connected. Shortest paths are more broadly defined, as common neighbors imply a path, but not vice versa. Moreover, since the embeddings of the nodes along the path are generated through message passing, they implicitly encode the broader local structure surrounding the link. This richer structural context enables SP4LP to distinguish non-automorphic links even when their endpoints are automorphic, thereby overcoming the automorphic node problem. We formally prove that SP4LP is strictly more expressive than several existing approaches.

SP4LP is **efficient** and **scalable**. The message-passing step is performed only once on the entire graph, and the shortest path computation is a preprocessing step. Unlike SF-then-GNN methods such as SEAL or NBFNet, SP4LP avoids costly per-link subgraph extraction or online traversal during inference, allowing it to scale to large graphs and high-throughput settings.

Moreover, SP4LP is a **general and flexible framework**. It can be instantiated with any GNN architecture to compute node embeddings (e.g., GCN [19], GAT [39], GraphSAGE [15]), and supports a range of sequence models for encoding the path structure, from lightweight aggregators to fully expressive recurrent or attention-based models.

Finally, SP4LP achieves **state-of-the-art performance** across several benchmark datasets. Under the challenging HeaRT evaluation protocol [24], it consistently outperforms existing link prediction methods while maintaining competitive inference speed and low memory usage.

These properties make SP4LP a principled and practical solution for learning expressive link representations in real-world graph learning scenarios.

2 Preliminaries

Definition 2.1 (*graph*)**.** A **graph** is a tuple $G = (V, E, \mathbf{X}^0)$ where $V = \{1, \ldots, n\}$ is a set of nodes, $E \subseteq V \times V$ is a set of edges and $\mathbf{X}^0 \in \mathbb{R}^{n \times f}$ is the node features matrix. To each graph is associated an adjacency matrix $\mathbf{A} \in \{0, 1\}^{n \times n}$ with $\mathbf{A}_{i,j} = 1$ if and only if $(i, j) \in E$. In this work, we consider simple, finite and undirected graphs.

Definition 2.2 (*message passing*)**.** Let $G = (V, E, \mathbf{X}^0)$ be a graph. In the **message passing** scheme, the representation of nodes $v \in V$ is iteratively updated as follows:

$$\mathbf{x}_v^0 = \mathbf{X}_{[v,:]}^0 \quad \mathbf{x}_v^l = \text{UPDATE}\left(\mathbf{x}_v^{l-1}, \text{AGGREGATE}\left(\{\mathbf{x}_u^{l-1} \mid u \in N(v)\}\right)\right) \tag{1}$$

where $N(v)$ is the first-order neighborhood of node v.

Graph Neural Networks (GNNs) are a class of neural architectures that operate on graphs by iteratively updating node representations through the message passing scheme. It has been proven that GNNs are at most as effective as the Weisfeiler–Lehman (WL) test in distinguishing between graphs [30, 43].

Definition 2.3 (GNN link representation model)**.** A **GNN link representation model** M is a class of functions

$$F : ((u, v), G) \mapsto \mathbf{x}_{(u,v)} \in \mathbb{R}^d \tag{2}$$

which maps node pairs in $(u, v) \in V \times V$ to vector representations using the message passing scheme defined in Definition 2.2.

Note that the pair (u, v) belongs to $V \times V$, meaning that we compute a representation for any node pair, what we refer to as a *link*, regardless of whether an edge between them exists in E. This general definition reflects the nature of the downstream tasks we aim to address once the link representation is available, most notably, link prediction, where the objective is to estimate the likelihood of a connection between arbitrary node pairs. To this end, the model learns representations for all possible pairs, not just those connected by an edge. A widely adopted approach for learning such representations is what we refer to as a *pure GNN*, defined as follows:

Definition 2.4 (*pure GNN*)**.** A **pure GNN** model calculates representation $\mathbf{x}_{(u,v)} \in \mathbb{R}^d$ for each pair of nodes (u, v) with $u, v \in V$ as follows:

$$\mathbf{x}_{(u,v)} = g(\mathbf{x}_u^L, \mathbf{x}_v^L) \tag{3}$$

where g is an aggregation function and $\mathbf{x}_u^L, \mathbf{x}_v^L$ are the node representation of u and v learned by L layers of message passing as defined in Definition 2.2.

Pure GNNs are inherently limited in terms of expressiveness. In particular even when the base GNN is the most powerful, they may assign the same representation to structurally different links. Consider, for example, the graph in Figure 1: the colors of the nodes indicate the colors produced by the WL algorithm; thus, using a most powerful GNN nodes u, u' will be assigned to the same representation. As a result, no matter how expressive the aggregation function g is, the representations of the pairs (v, u) and (v, u') will be identical. However, the links (v, u) and (v, u') have different roles within the graph structure. We provide a formal definition of what it means for two links to be different.

Definition 2.5 (*node permutation*)**.** A **node permutation** $\pi : \{1, \dots, n\} \to \{1, \dots, n\}$ is a bijective function that assigns a new index to each node of the graph. All the $n!$ possible node permutations constitute the permutation group Π_n. Given a subset of nodes $S \subseteq V$, we define the permutation π on S as $\pi(S) := \{\pi(i) | i \in S\}$. Additionally, we define $\pi(\mathbf{A})$ as the matrix $\mathbf{A}$ with rows and columns permutated based on π, i.e., $\pi(\mathbf{A})_{\pi(i),\pi(j)} = \mathbf{A}_{i,j}$.

Definition 2.6 (*automorphism*)**.** An **automorphism** on the graph $G = (V, E, \mathbf{X}^0)$ is a permutation $\sigma \in \Pi_n$ such that $\sigma(\mathbf{A}) = \mathbf{A}$ and $\mathbf{X}^0_{\sigma(i),:} = \mathbf{X}^0_{i,:}$ for every $i \in V$. All such feature-preserving automorphisms constitute the automorphism group Σ_n^G. For constant node features, this reduces to the usual structural automorphism group.

Definition 2.7 (*automorphic nodes*)**.** Let $G = (V, E, \mathbf{X}^0)$ be a graph and Σ_n^G its automorphism group. Two nodes $u, v \in V$ are said to be **automorphic nodes** ($u \simeq v$) if:

$$\exists \sigma \in \Sigma_n^G \quad \text{s.t.} \quad \sigma(\{u\}) = \{v\}. \tag{4}$$

Definition 2.8 (*automorphic links*)**.** Let $G = (V, E, \mathbf{X}^0)$ be a graph and Σ_n^G its automorphism group. Two pairs of nodes $(u, v), (u', v') \in V \times V$ are said to be **automorphic links** ($(u, v) \simeq (u', v')$) if:

$$\exists \sigma \in \Sigma_n^G \quad \text{s.t.} \quad \sigma(\{u, v\}) = \{u', v'\}. \tag{5}$$

Proposition 2.9. *Pure GNN methods suffer from the automorphic node problem, i.e., for any graph $G = (V, E, \mathbf{X}^0)$, for pairs of links $(u, v), (u', v') \in V \times V$ such that there exist $\sigma_1 \in \Sigma_n^G$ and $\sigma_2 \in \Sigma_n^G$ with $\sigma_1(u) = u'$ and $\sigma_2(v) = v'$, $\mathbf{x}_{(u,v)} = \mathbf{x}_{(u',v')}$, independently of whether (u, v) and (u', v') are isomorphic, i.e, whether there exists $\sigma \in \Sigma_n^G$ with $\sigma(\{u, v\}) = \{u', v'\}$.*

This limitation is well-known in the literature [4, 49]. Importantly, it does not arise from the expressiveness bounds of GNNs, which are constrained by the WL test. Even considering higher-order GNNs, i.e., k-GNN [30], automorphic nodes will be assigned to the same representation as the

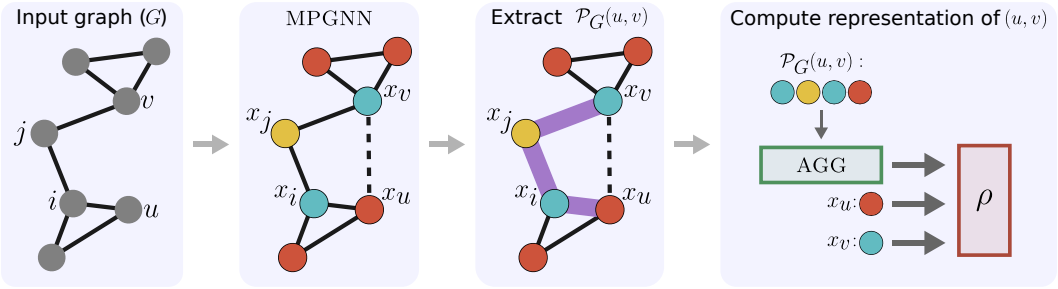

Figure 2: Overview of the SP4LP framework. First, a GNN is used to compute contextualized embeddings for all nodes in the graph. Then, for each target link, the shortest path connecting the two endpoints is extracted. The embeddings of the nodes along this path are passed to a sequence model (e.g., Transformer or LSTM) to compute a path-aware link representation.

k-WL algorithm preserves graph automorphisms for every k [3, 10, 26]. Thus, no standard GNN can distinguish non automorphic links composed by automorphic nodes.

To tackle this, several models have been proposed that enhance message passing by incorporating structural features [4, 40, 42, 49, 52], thereby increasing the expressive power of the resulting link representations. We provide a formal definition of what it means for one link representation model to be more expressive and strictly more expressive than another.

Definition 2.10 (*more expressive*)**.** Let $\mathcal{M}_1$ and $\mathcal{M}_2$ be two link representation models (Def. 2.3). $\mathcal{M}_2$ is **more expressive** than $\mathcal{M}_1$ ($\mathcal{M}_1 \preceq \mathcal{M}_2$) if, for any graph $G = (V, E, \mathbf{X}^0)$ and any pair $(u, v), (u', v') \in V \times V$ with $(u, v) \not\simeq (u', v')$:

$$\exists F_1 \in \mathcal{M}_1 : \; F_1((u,v), G) \neq F_1((u',v'), G) \;\Rightarrow \exists F_2 \in \mathcal{M}_2 : \; F_2((u,v), G) \neq F_2((u',v'), G). \tag{6}$$

Definition 2.11 (*strictly more expressive*)**.** Let $\mathcal{M}_1$ and $\mathcal{M}_2$ be two link representation models (Def. 2.3). We say that $\mathcal{M}_2$ is **strictly more expressive** than $\mathcal{M}_1$ ($\mathcal{M}_1 \prec \mathcal{M}_2$) if:

- $\mathcal{M}_2$ is more expressive than $\mathcal{M}_1$ (Def. 2.10), and
- there exists a graph $G = (V, E, \mathbf{X}^0)$ and a pair of links $(u, v), (u', v') \in V \times V$ with $(u, v) \not\simeq (u', v')$ such that:

$$\begin{aligned} &\forall F_1 \in \mathcal{M}_1 : \quad F_1((u,v), G) = F_1((u',v'), G) \\ \text{and} \quad &\exists F_2 \in \mathcal{M}_2 : \quad F_2((u,v), G) \neq F_2((u',v'), G). \end{aligned}$$

In section 4 we introduce our model SP4LP and demonstrate its improved expressive power in distinguishing structurally different links.

3 Related Work

GNNs have been extensively used for link representation tasks. In standard approaches like Graph Autoencoders (GAE) [20], node embeddings are computed via message passing, and a simple decoder (e.g., inner product followed by a sigmoid) predicts link existence. While efficient, these models exhibit limited expressiveness [4, 49], primarily due to their inability to capture rich structural patterns beyond immediate neighborhoods. This limitation has motivated the integration of explicit structural information into GNN-based models. An alternative approach [22], learns structural link representations by reformulating link prediction as node classification on a line graph.

Incorporating Structural Information into GNNs. Several methods inject structural information into GNN-based link predictors to overcome expressiveness bottlenecks. Neo-GNN [47] adds handcrafted structural signals to aggregation, while ELPH [4] and its scalable variant BUDDY encode multi-hop neighborhood patterns via MinHash and HyperLogLog sketches, precomputed offline in BUDDY for efficiency. MPLP [12] replaces sketching with message passing over quasi-orthogonal random vectors, yielding unbiased estimates of common neighbor counts and Distance Encoding

labels concatenated with GNN embeddings. NCN [42] aggregates embeddings from endpoints and their common neighbors, and NCNC extends it by first predicting missing neighbors. NBFNet [52] instead aggregates over all node-pair paths via Bellman–Ford-inspired recursive updates. Beyond GNNs, PROXI [36] combines handcrafted proximity indices with XGBoost; while related through its use of structural signals, it fundamentally differs from GNN-based link representation models. Despite these advances, such mechanisms still struggle to distinguish more complex structures, as shown in the next section.

Enhancing GNN Expressiveness through Positional and Structural Encoding. Positional encodings further enrich GNN expressiveness. PEG [40] integrates Laplacian-based encodings into message passing, weighting neighbors by positional distances. SEAL [49] extracts h-hop enclosing subgraphs and labels nodes via the DRNL scheme before applying a GNN. While expressive, these methods struggle to scale due to subgraph extraction overhead. In contrast, our model achieves expressiveness by operating directly on compact, informative shortest-path sequences, enabling better scalability without sacrificing representational power.

Shortest-Path and Path-Based Methods in Graph Learning. Path-based representations have a long history in graph learning, from shortest-path kernels [2] to recent neural approaches that aggregate information over walks or simple paths for graph- and node-level tasks [5, 6, 29, 45], and to generative graph transformers built on Eulerian path linearizations [50]. Within link prediction, Geodesic GNN (GDGNN) [21] aggregates node representations along geodesic connections after global message passing, typically using permutation-invariant aggregation that abstracts away ordering. In contrast, SP4LP is pair-centric and explicitly models the shortest path between two endpoints as a learnable ordered sequence, yielding link representations that capture directional and positional structure. Recent results [1] further show that walk-based encodings can fail to distinguish node pairs that path-based representations separate.

4 SP4LP: An Expressive GNN-then-SF Model for link Representation

Existing GNN link representation models that leverage Structural Features (SF) fall into three categories [42]: **SF-and-GNN**, which compute SF and GNN embeddings separately and then combine them (e.g., Neo-GNN [47], BUDDY [4]); **SF-then-GNN**, which augment the graph with SF before applying GNN (e.g., SEAL [48], NBFNet [52]); and **GNN-then-SF**, which compute GNN embeddings first and then aggregate them using SF (e.g., NCN, NCNC [42]).

In this work, we adopt the GNN-then-SF paradigm, which combines the scalability advantages of applying message passing only once, as in the SF-and-GNN setting, with the expressiveness typical of SF-then-GNN approaches, due to the ability to aggregate over task-specific sets of node representations. To date, the only existing models that follow this paradigm are NCN and NCNC. For a more in-depth discussion on the differences between our method, SP4LP and NCN, refer to Section 4.1. In the following, we introduce the necessary definitions, formally describe the model, and present theoretical results characterizing its expressive power.

Definition 4.1 (*path*)**.** Let $G = (V, E, \mathbf{X}^0)$ be a graph and $u, v \in V$ to nodes. A **path** in G from u to v is a sequence of nodes $P = (u_0, u_1, \ldots, u_k)$ with (i) $u_i \in V$ for all $i = 0, \ldots, k-1$, (ii) $u_0 = u$ and $u_k = v$, (iii) $(u_i, u_{i+1}) \in E$ for all $i = 0, \ldots, k-1$, and (iv) all nodes in the sequence are distinct (i.e., $u_i \neq u_j$ for all $i \neq j$). The length of a path P, $\text{len}(P)$ is the number of edges it contains.

Definition 4.2 (*shortest path length*)**.** Let $\mathcal{P}_G(u, v)$ denote the set of all paths from u to v in G. The **shortest path length** $d_G(u, v)$ is the minimum length among all paths i.e., $d_G(u, v) = \min_{P \in \mathcal{P}(u,v)} \text{len}(P)$.

Definition 4.3 (*shortest path*)**.** A **shortest path** between u to v in G is any path $P^* \in \mathcal{P}_G(u, v)$ such that $\text{len}(P^*) = d_G(u, v)$. The set of all the shortest path from u to v in G is denoted as $\mathcal{P}^*_G(u, v)$.

Let $G = (V, E, \mathbf{X}^0)$ be a graph, $u, v \in V$. SP4LP is a GNN link representation model (see Definition 2.3) that computes link representation as follows:

$$\text{SP4LP}((u, v), G) = \rho\left(\text{GNN}(u, G), \text{GNN}(v, G), \text{AGG}\left(\left\{\phi\left((\text{GNN}(u_i, G))_{i=0}^k\right) \mid (u_i)_{i=0}^k \in \mathcal{P}^*_G\{u, v\}\right\}\right)\right) \tag{7}$$

where $k = d_G(u, v)$, $\text{GNN}(u, G) \in \mathbb{R}^d$ is the representation of node $u \in V$ obtained at the final layer of message passing as in Definition 2.2, $\phi : \bigcup_{\ell \geq 1} (\mathbb{R}^d)^\ell \to \mathbb{R}^d$ is a sequence encoder operating on the full ordered sequence of node embeddings along the shortest path from u to v, including both endpoints, AGG is an aggregation function over multiset of shortest paths representations and $\rho : \mathbb{R}^d \times \mathbb{R}^d \times \mathbb{R}^d \to \mathbb{R}^d$ combine the endpoint nodes representations with the shortest paths representation to get a final link representation. Since we consider undirected graphs, we consider $\mathcal{P}^*_G\{u, v\} := \mathcal{P}^*_G(u, v) \cup \mathcal{P}^*_G(v, u)$. For disconnected pairs, $d_G(u, v) = +\infty$ and no shortest path exists. In this case, we use the endpoint-only sequence (u, v) as a fallback input to the path encoder, with no additional no-path token. This sequence is not a graph path: the path branch uses only the two endpoint GNN embeddings, without intermediate nodes.

Although shortest paths provide a focused and efficient structural summary, they may lose information carried by alternative routes or larger subgraphs, reducing robustness and emphasizing local rather than global structure. We quantify this trade-off experimentally in Section 5.1, showing that replacing full path embeddings with simple distance information leads to significant performance degradation.

For a graph with n nodes and m edges, single-source BFS [9] runs in $O(n+m)$ time on an adjacency-list representation. Although computing all-pairs shortest paths (APSP) would require $O(n(n + m))$ time, SP4LP does not perform APSP. In our experiments, we compute shortest paths only for the supervised train/validation/test links, which requires at most a small number of BFS traversals. Let S be the number of distinct source nodes among these links; the preprocessing cost is therefore $O(S(n + m))$, typically several orders of magnitude smaller than $O(n(n + m))$. The resulting paths are cached and reused throughout training and inference, so no graph traversal is performed during model training or batched evaluation. In fully-inductive settings where new nodes may appear, one can compute shortest-path trees by running a single BFS per new node, providing distances and parent pointers to all existing nodes at once. This preserves the same per-link inference efficiency and avoids BFS operations per queried link. A more detailed analysis of the overall complexity, including a comparison with prior approaches, is provided in Appendix E. In practice, all shortest paths are precomputed before training, and SP4LP simply retrieves the stored sequences during training and inference. No BFS operations are performed online.

SP4LP is a general and flexible framework: both the underlying GNN used to compute node representations and the sequence model used to process the embeddings along the shortest path can be chosen modularly. For instance, the GNN component can be instantiated with architectures such as GCN [19], GAT [38] or GraphSAGE [15], while the sequence model can range from simple aggregation functions like injective summation as the one proposed in Xu et al. [43], to more complex architectures such as LSTMs [16], GRU [8] or Transformers [37]. An overview of SP4LP is illustrated in Figure 2.

The additional structural context given by the sequence of embeddings of nodes within the shortest path enables the model to distinguish links that are otherwise indistinguishable to standard message-passing methods, such as those involving automorphic nodes.

Proposition 4.4. SP4LP *does not suffer from the automorphic node problem.*

The proof constructs two non-automorphic links with automorphic corresponding endpoints. Pure endpoint-based GNN models assign them identical representations, whereas their different shortest-path lengths allow a suitable instantiation of SP4LP to distinguish them. The complete proof is provided in Appendix A. As an example of non-automorphic links composed of automorphic nodes that SP4LP can successfully distinguish, consider the links (v, u) and (v, u') shown in Figure 1. The two links have automorphic corresponding endpoints: $v \simeq v$ via the identity and $u \simeq u'$ via a feature-preserving graph automorphism. However, the links (v, u) and (v, u') are not automorphic, since their endpoints have different shortest-path distances. This asymmetry is captured by the distinct shortest paths between the endpoints: the shortest path from v to u' consists of v, and orange node, and u', whereas the shortest path from v to u includes v, and orange node, a yellow node, another orange node, and finally u. This example also defines an interpretable synthetic classification task: distinguish the same-side pair (v, u') from the cross-graph pair (v, u) across randomly relabeled copies of the graph, preserving node features. A pure endpoint-based GNN assigns identical representations to the two pairs and therefore cannot distinguish their classes. In contrast, a suitable instantiation of SP4LP can separate them through their different shortest-path lengths. This is a representational comparison, rather than an empirical evaluation of training or generalization. In addition to overcoming this limitation, SP4LP is strictly more expressive than several state-of-the-art message passing methods

for link representation learning. The comparison with NCN assumes that the queried edge is removed, if present, and that both models use the resulting graph for message passing and structural feature extraction. It concerns the general SP4LP formulation aggregating all shortest paths, rather than the single-path implementation used in our experiments.

Theorem 4.5. SP4LP *is strictly more expressive than pure GNN link representation models, NCN, the set-based horizontal GDGNN link encoder, and the degree-free vertical GDGNN link encoder. Moreover, neither Neo-GNN nor BUDDY is more expressive than* SP4LP.

For each baseline covered by the strict expressiveness claim, the proof first shows how an appropriate choice of ϕ, AGG, and ρ reproduces its link representation under the stated assumptions. Strictness follows from examples of links that the baseline cannot distinguish but SP4LP separates using path length, internal-node information, or node order. The non-domination result for Neo-GNN and BUDDY follows from the NCN comparison by transitivity. The complete proof is provided in Appendix A. In the following sections, we complement the theoretical analysis with an extensive experimental evaluation, showing that SP4LP also achieves state-of-the-art performance on standard link prediction benchmarks.

4.1 Further comparison with NCN

NCN represents a link by aggregating the GNN embeddings of its endpoints and their common neighbors, making it particularly vulnerable to graph incompleteness. When two endpoints share no neighbors, NCN reduces to a pure GNN and can no longer leverage structural information, a far from rare situation in practice: the fraction of positive test links without common neighbors reaches 46%, 55%, and 67% on Cora, Citeseer, and Pubmed, and 10%, 37%, and 52% on ogbl-ppa, ogbl-citation2, and ogbl-collab (only ogbl-ddi is unaffected, at 0.04%). In contrast, SP4LP encodes the sequence of node embeddings along the shortest path between endpoints, which is always defined in connected graphs and captures richer structural patterns even in sparse or incomplete settings. Moreover, while NCN pools neighbors as unordered sets, SP4LP encodes paths as ordered sequences via LSTMs or Transformers, yielding strictly higher expressiveness (Theorem 4.5).

5 Experiments

We evaluate SP4LP on real-world link prediction benchmarks, where observed edges are treated as positive examples and non-edges, sampled via negative sampling, as negatives. We consider three Planetoid citation networks, Cora, Citeseer, and Pubmed [44], and four OGB datasets, ogbl-citation2, ogbl-ppa, ogbl-collab and ogbl-ddi [17]. For the Planetoid datasets, we use a single fixed split across all experiments. Dataset statistics are reported in Table 8 of section C.

As baseline methods we consider **Pure GNN methods**: Graph Convolutional Network (GCN) [19], Graph Attention Network (GAT) [39], GraphSAGE [15], and Graph Autoencoder (GAE) [20], and **Structural Features GNN methods**: SEAL [48], BUDDY [4], Neo-GNN [47], NBFNet [52], NCN [42], NCNC [42] and PEG [40], GDGNN [21], MPLP [12]. We additionally evaluate two recent link prediction models that fall outside the message-passing taxonomy of Section 3: LPFormer [33], a transformer-based model with attention over node-pair contexts, and GraphGPT [50], a generative graph transformer that linearizes graphs via Eulerian paths.

As described in Section 4, SP4LP is a general framework that supports different choices of GNN backbone and sequence model ϕ (Equation 7), both treated as hyperparameters and tuned on the validation set. We explore GCN, GAT, and GraphSAGE as backbones, and LSTM, Transformer, and an injective sum aggregator [43] as sequence models. We use an MLP for ρ and, for efficiency, select the first shortest path returned by BFS as AGG. Appendix D reports implementation details, shortest-path computation, and hyperparameter configurations. Code is available at[2]

Evaluation Setting We evaluate model performance under the more challenging and realistic HeaRT evaluation setting [24]. In this setting, each positive target link (i.e., an existing link) is ranked against a carefully selected set of hard negative samples (i.e., non-existing links), providing a more realistic assessment of link prediction performance in practical scenarios. We adopt two standard ranking metrics: Hits@K and Mean Reciprocal Rank (MRR). Following the HeaRT protocol,

[2] https://github.com/francescoferrini/sp4lp

Table 1: MRR and Hits@K (%) on citation (Cora, Citeseer, Pubmed) and OGB benchmarks, following the HeaRT evaluation setting [24]. Hits@10 is reported for citation datasets and Hits@20 for OGB. Top three results per metric are highlighted as **first**, **second**, **third**. *OOM* = out of memory; *>24h* = did not complete within 24 hours. Methods are grouped into pure GNN baselines (**GNN**), GNNs augmented with structural features (**SF GNN**), and graph transformers (**GT**). Standard deviations over 5 runs are in section B. Note: GDGNN's original paper reports OGB results under a different protocol that does not follow HeaRT (which uses harder negative sampling and is significantly more expensive).

	Models	Cora		Citeseer		Pubmed		Ogbl-ddi		Ogbl-collab		Ogbl-ppa		Ogbl-citation2	
		MRR	H@10	MRR	H@10	MRR	H@10	MRR	H@20	MRR	H@20	MRR	H@20	MRR	H@20
GNN	GCN	16.61	36.26	21.09	47.23	7.13	15.22	**13.46**	64.76	6.09	**22.48**	26.94	68.38	19.98	51.72
GNN	GAT	13.84	32.89	19.58	45.30	4.95	9.99	12.92	**66.83**	4.18	18.30	*OOM*	*OOM*	*OOM*	*OOM*
GNN	SAGE	14.74	34.65	21.09	48.75	**9.40**	**20.54**	12.60	**67.19**	5.53	21.26	27.27	69.49	22.05	53.13
GNN	GAE	**18.32**	**37.95**	25.25	49.65	5.27	10.50	3.49	17.81	*OOM*	*OOM*	*OOM*	*OOM*	*OOM*	*OOM*
GT	LPFORMER	**16.80**	34.03	**26.34**	**51.72**	**9.99**	**21.43**	13.20	62.66	**7.62**	21.04	**40.25**	**84.10**	**24.70**	**57.30**
GT	GraphGPT	8.07	18.03	8.72	19.78	3.18	5.98	*>24h*	*>24h*	1.73	6.24	*>24h*	*>24h*	*>24h*	*>24h*
SF GNN	GDGNN	6.32	15.97	7.93	14.25	0.96	1.10	*>24h*	*>24h*	*>24h*	*>24h*	*>24h*	*>24h*	*>24h*	*>24h*
SF GNN	SEAL	10.67	24.27	13.16	27.37	5.88	12.47	9.99	49.74	6.43	21.57	29.71	76.77	20.60	48.62
SF GNN	BUDDY	13.71	30.40	22.84	48.35	7.56	16.78	12.43	58.71	5.67	**23.35**	27.70	71.50	19.17	47.81
SF GNN	Neo-GNN	13.95	31.27	17.34	41.74	7.74	17.88	10.86	51.94	5.23	21.03	21.68	64.81	16.12	43.17
SF GNN	NCN	14.66	35.14	**28.65**	**53.41**	5.84	13.22	12.86	**65.82**	5.09	20.84	35.06	81.89	**23.35**	53.76
SF GNN	NCNC	14.98	**36.70**	24.10	**53.72**	8.58	18.81	*>24h*	*>24h*	4.73	20.49	33.52	**82.24**	19.61	51.69
SF GNN	NBFNet	13.56	31.12	14.29	31.39	*>24h*	*>24h*	*>24h*	*>24h*	*OOM*	*OOM*	*OOM*	*OOM*	*OOM*	*OOM*
SF GNN	PEG	15.73	36.03	21.01	45.56	4.40	8.70	12.05	50.12	4.83	18.29	*OOM*	*OOM*	*OOM*	*OOM*
SF GNN	MPLP	12.57	27.70	12.55	27.33	5.19	10.97	**13.94**	59.17	**6.79**	**25.10**	**41.40**	**84.80**	23.11	**55.51**
	SP4LP (our)	**28.84**	**45.39**	**29.48**	49.52	**10.87**	**23.01**	**15.00**	47.96	**9.46**	20.00	**36.45**	76.90	**24.91**	**55.45**

we report Hits@10 and MRR for Cora, Citeseer, and Pubmed, and Hits@20 along with MRR for ogbl-collab, ogbl-ddi, ogbl-ppa and ogbl-citation2. The same set of negative samples is used across all positive links, as specified in the HeaRT benchmark. The HeaRT evaluation introduces significantly harder negative samples compared to traditional evaluation settings, resulting in a more challenging and realistic benchmark. Li et al. [24] show that this leads to a substantial performance drop across most models, with GNNs specifically designed for link prediction often being outperformed by simple heuristics or general-purpose GNNs. By adopting this challenging setting, we ensure a rigorous and meaningful comparison of model performance under conditions that closely resemble real-world applications.

Table 1 presents the performance of SP4LP and the baseline models in terms of MRR and Hits@10 on Cora, Citeseer, and Pubmed, and MRR and Hits@20 on the OGB datasets. SP4LP ranks first in terms of MRR on six out of seven datasets and third on the remaining one. The improvements in MRR are often substantial: on Cora, for instance, SP4LP achieves a 57% gain over the second-best method, GAE, and on Ogbl-Collab a 24% gain over the second-best method, LPFormer, highlighting a markedly stronger empirical predictive capability of our approach. SP4LP also achieves the best Hits@K score on Cora and Pubmed, and ranks among the top three on Ogbl-Citation2. On Ogbl-Collab, although SP4LP does not rank among the top performers on Hits@20, it remains comparable to several baselines (e.g., NCN, NCNC, Neo-GNN) when accounting for standard deviations (Appendix B). MRR and Hits@K capture different aspects of ranking quality: moving a positive link from rank 10 to rank 2 improves MRR without changing Hits@20. Thus, the MRR gains of SP4LP need not translate into higher top-20 coverage. On ogbl-ddi, shortest paths have average length approximately two, and only 0.04% of positive test links lack common neighbors, limiting the additional structural information provided by a single path. On ogbl-collab and ogbl-ppa, selecting one shortest path may likewise discard evidence distributed across multiple paths or common neighbors. Greater theoretical expressiveness therefore does not guarantee improvements on every metric: empirical performance also depends on graph structure, optimization, and architectural inductive bias. In addition to achieving the best performance in several datasets, SP4LP is also the most consistent model across all benchmarks. Unlike previous state-of-the-art models such as BUDDY and Neo-GNN, which tend to struggle on datasets like Cora, Citeseer and Pubmed, SP4LP maintains strong performance regardless of dataset characteristics. Overall, these results clearly demonstrate the superiority of SP4LP under the more challenging and realistic HeaRT evaluation setting, confirming its effectiveness for real-world link prediction tasks.

5.1 Ablation Study

Table 2: Ablation study results (%). MRR and Hits@K are reported for two model variants: (1) *Sequence Model Only*, and (2) *GNN + Shortest Path Length*. The full model SP4LP consistently outperforms both variants.

Models	Cora		Citeseer		Pubmed	
	MRR	H@10	MRR	H@10	MRR	H@10
GNN + SP	8.32	20.02	21.13	45.05	8.52	15.32
Seq. Model	16.86	36.03	10.93	19.23	7.12	13.56
SP4LP	**28.84**	**45.39**	**29.48**	**49.52**	**10.87**	**23.01**

We perform an ablation study to evaluate the contribution of the main components of our model. In particular, we investigate two simplified variants to understand the importance of node representation learning and sequential modeling along the shortest path between target nodes. **(1) Sequence Model Only**: in this variant, the sequential model operates directly on the raw input features of the nodes along the shortest path, without incorporating node representations learned by the GNN. This setup isolates the contribution of the sequential model in capturing relational patterns based solely on node features and structural path information. **(2) GNN + Shortest Path Length:** in this variant, the sequential model is completely removed. Link prediction is performed using only the learned node representations from the GNN, combined with the length of the shortest path between the target nodes. This evaluates the effectiveness of combining node embeddings with simple distance information, without explicitly modeling the intermediate nodes along the path.

Table 2 reports the results of these ablations on Cora, Citeseer, and Pubmed. Both variants show a clear performance drop compared to the full model, demonstrating the importance of jointly leveraging node representations and sequential modeling. Note that, since both variants inherit the GNN configuration optimized for the full SP4LP pipeline rather than being independently retuned, their absolute scores are not directly comparable to the standalone GNN baselines in Table 1; the meaningful comparison is between each variant and the full SP4LP. The relative ranking of the two variants is dataset-dependent: Sequence Model Only performs better on Cora, while GNN + Shortest Path Length is stronger on Citeseer and Pubmed. In all cases, neither variant approaches the full SP4LP: replacing the path embedding with its length discards the information carried by node representations along the path, while operating on raw features deprives the model of the broader structural context implicitly encoded by message passing. The full SP4LP consistently achieves the best results across all datasets, confirming the importance of combining learned node representations with sequential modeling over the shortest paths.

The ablation results also suggest that joint optimization of the GNN and sequence encoder contributes to the variability observed on the smaller datasets. On Cora, the MRR standard deviation increases from 0.28 for GNN + shortest-path length and 1.26 for the sequence-only model to 5.45 for the full model. On Citeseer, the corresponding values are 0.99, 2.93, and 10.17. Hits@10 exhibits the same pattern (Appendix B, Table 5). These observations suggest an interaction between the two components, rather than establishing a definitive cause of the variability.

5.2 Scalability Analysis

We assess the scalability of SP4LP by examining how its GPU memory consumption and inference time evolve as the batch size increases, in comparison to several baseline methods. The results are presented in Figure 3. In terms of GPU memory usage, SP4LP exhibits remarkable efficiency: memory consumption remains nearly constant across small to medium batch sizes, and increases moderately only for the largest batches, starting with 0.77 GB and reaching at most 6.84 GB while consistently avoiding out-of-memory (OOM) failures.

PEG also maintains low memory usage; however, this advantage is undermined by its impractically slow inference, limiting its applicability in large-scale scenarios. SEAL, while competitive with SP4LP in terms of inference speed, suffers from excessive memory consumption, rapidly exceeding 18 GB and encountering OOM issues beyond a batch size of 32,768. NCNC is even more constrained, experiencing OOM failures already at relatively small batch sizes. Considering inference time, SP4LP matches the efficiency of SEAL, requiring only 2.1 seconds for o batch size of 16,384 and scaling smoothly to 4.29 seconds at 65,536. PEG, by contrast, is significantly slower, already taking 5 seconds at a batch size of 8,192 and exceeding 23 seconds at the maximum batch size tested. Although NCN and Buddy consistently achieve low inference times, this comes at the cost of substantially lower predictive performance, as they rely on simple heuristics with limited modeling

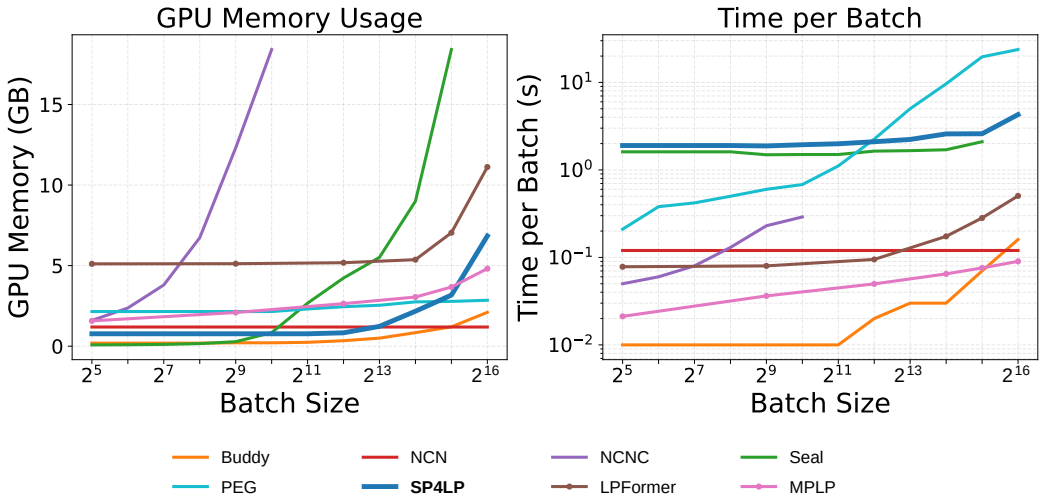

Figure 3: Inference time and GPU memory usage on ogbl-collab, measured during the prediction of a single batch of test links. GDGNN is omitted because it did not complete within 24 hours. GraphGPT is omitted because its autoregressive decoding over variable-length sequences is not directly comparable to the batch-forward inference measured here.

capacity. This trade-off is clearly reflected in the results of Table 1. LPFormer and MPLP achieve lower inference times than SP4LP at the measured batch sizes. At batch size 65,536, their GPU memory usage is 11.12 GB and 4.81 GB, respectively, compared with 6.84 GB for SP4LP. These results show a trade-off: SP4LP achieves higher MRR on ogbl-collab, while these baselines offer faster inference.

6 Conclusion

We introduced SP4LP, a message-passing framework for link representation that enhances the expressiveness of standard GNNs by incorporating sequential modeling over the shortest path between target nodes. Following the GNN-then-SF paradigm, SP4LP combines the efficiency of computing node embeddings only once with high expressive power, explicitly modeling multi-hop relational patterns via a sequence encoder applied to node embeddings along the shortest path. We formally proved that SP4LP is strictly more expressive than several state-of-the-art link representation models, and extensive experiments under the HeaRT evaluation protocol confirm that it achieves state-of-the-art performance across diverse datasets.

Limitations. SP4LP presents two main limitations. First, it requires a preprocessing step to compute and cache shortest paths, which adds complexity compared to fully end-to-end models, although this cost is amortized across training and inference. Second, SP4LP's advantage is reduced on graphs with very short average shortest-path length (e.g., ogbl-ddi, with average length ≈ 2), where path-based modeling has limited room to exploit structural information beyond what local methods already capture.

Future work. We plan to extend SP4LP in several directions: incorporating multiple (or all) shortest paths to improve robustness and capture richer structural signals; adapting SP4LP to heterogeneous graphs [13], where shortest paths remain well-defined and the path encoder can naturally incorporate node and edge type embeddings; and extending our preliminary analysis of truncated BFS to larger graphs and other approximation techniques, such as landmark-based methods, to reduce preprocessing cost.

Acknowledgments

FF, BL, and AP were funded by the European Union under Grant Agreement No. 101120763 (TANGO), and Grant Agreement No. 101120237 (ELIAS). FF and BL were funded by Horizon Europe Grant Agreement No. 101297599 (EURO-3C). AL and VL were funded by the Research Council of Norway through its Centre of Excellence Integreat – The Norwegian Centre for Knowledge-Driven Machine Learning (project no. 332645). Views and opinions expressed are however those of the author(s) only and do not necessarily reflect those of the European Union or the European Health and Digital Executive Agency (HaDEA). Neither the European Union nor the granting authorities can be held responsible for them.

References

[1] Airale, L., Longa, A., Rigon, M., Passerini, A., and Passerone, R. Simple path structural encoding for graph transformers. In *Forty-second International Conference on Machine Learning*, 2025. URL https://openreview.net/forum?id=t3zwUqibMq.

[2] Borgwardt, K. M. and Kriegel, H.-P. Shortest-path kernels on graphs. In *Fifth IEEE international conference on data mining (ICDM'05)*, pp. 8–pp. IEEE, 2005.

[3] Cai, J.-Y., Fürer, M., and Immerman, N. An optimal lower bound on the number of variables for graph identification. *Combinatorica*, 12(4):389–410, 1992.

[4] Chamberlain, B. P., Shirobokov, S., Rossi, E., Frasca, F., Markovich, T., Hammerla, N. Y., Bronstein, M. M., and Hansmire, M. Graph neural networks for link prediction with subgraph sketching. In *The Eleventh International Conference on Learning Representations*, 2023. URL https://openreview.net/forum?id=m1oqEOAozQU.

[5] Chen, D., Jacob, L., and Mairal, J. Convolutional kernel networks for graph-structured data. In *international conference on machine learning*, pp. 1576–1586. PMLR, 2020.

[6] Chen, D., Schulz, T. H., and Borgwardt, K. Learning long range dependencies on graphs via random walks. *arXiv preprint arXiv:2406.03386*, 2024.

[7] Cheng, X., Wang, Y., Liu, Y., Zhao, Y., Aggarwal, C. C., and Derr, T. Edge classification on graphs: New directions in topological imbalance. In *Proceedings of the Eighteenth ACM International Conference on Web Search and Data Mining*, pp. 392–400, 2025.

[8] Chung, J., Gulcehre, C., Cho, K., and Bengio, Y. Empirical evaluation of gated recurrent neural networks on sequence modeling. *arXiv preprint arXiv:1412.3555*, 2014.

[9] Cormen, T. H., Leiserson, C. E., Rivest, R. L., and Stein, C. *Introduction to Algorithms*. MIT Press, Cambridge, MA, 3rd edition, 2009.

[10] Dawar, A. and Vagnozzi, D. Generalizations of k-dimensional weisfeiler–leman stabilization. *Moscow Journal of Combinatorics and Number Theory*, 9(3):229–252, 2020.

[11] Dong, B., Aggarwal, C. C., and Philip, S. Y. The link regression problem in graph streams. In *2019 IEEE International Conference on Big Data (Big Data)*, pp. 1088–1095. IEEE, 2019.

[12] Dong, K., Guo, Z., and Chawla, N. V. Pure message passing can estimate common neighbor for link prediction. In *The Thirty-eighth Annual Conference on Neural Information Processing Systems*, 2024. URL https://openreview.net/forum?id=Xa3dVaolKo.

[13] Ferrini, F., Longa, A., Passerini, A., and Jaeger, M. A self-explainable heterogeneous GNN for relational deep learning. *Transactions on Machine Learning Research*, 2025. ISSN 2835-8856. URL https://openreview.net/forum?id=8Q4qxe9a9Z.

[14] Hagberg, A., Swart, P. J., and Schult, D. A. Exploring network structure, dynamics, and function using networkx. Technical report, Los Alamos National Laboratory (LANL), Los Alamos, NM (United States), 2008.

[15] Hamilton, W., Ying, Z., and Leskovec, J. Inductive representation learning on large graphs. *Advances in neural information processing systems*, 30, 2017.

[16] Hochreiter, S. and Schmidhuber, J. Long short-term memory. *Neural computation*, 9(8): 1735–1780, 1997.

[17] Hu, W., Fey, M., Zitnik, M., Dong, Y., Ren, H., Liu, B., Catasta, M., and Leskovec, J. Open graph benchmark: Datasets for machine learning on graphs. *Advances in neural information processing systems*, 33:22118–22133, 2020.

[18] Jha, K., Saha, S., and Singh, H. Prediction of protein–protein interaction using graph neural networks. *Scientific Reports*, 12(1):8360, 2022.

[19] Kipf, T. N. and Welling, M. Semi-supervised classification with graph convolutional networks. *arXiv preprint arXiv:1609.02907*, 2016.

[20] Kipf, T. N. and Welling, M. Variational graph auto-encoders. *arXiv preprint arXiv:1611.07308*, 2016.

[21] Kong, L., Chen, Y., and Zhang, M. Geodesic graph neural network for efficient graph representation learning. *Advances in neural information processing systems*, 35:5896–5909, 2022.

[22] Lachi, V., Ferrini, F., Longa, A., Lepri, B., and Passerini, A. A simple and expressive graph neural network based method for structural link representation. In *ICML 2024 Workshop on Geometry-grounded Representation Learning and Generative Modeling*, 2024. URL https://openreview.net/forum?id=EGGSCLyVrz.

[23] Lachi, V., Ferrini, F., Longa, A., Lepri, B., Passerini, A., and Jaeger, M. Bridging theory and practice in link representation with graph neural networks. In Belgrave, D., Zhang, C., Lin, H., Pascanu, R., Koniusz, P., Ghassemi, M., and Chen, N. (eds.), *Advances in Neural Information Processing Systems*, volume 38, Main Conference, pp. 122617–122646. Curran Associates, Inc., 2025. doi: 10.52202/085713-4090. URL https://proceedings.neurips.cc/paper_files/paper/2025/file/b1cd72276feff8173462e3f733ac66f8-Paper-Conference.pdf.

[24] Li, J., Shomer, H., Mao, H., Zeng, S., Ma, Y., Shah, N., Tang, J., and Yin, D. Evaluating graph neural networks for link prediction: Current pitfalls and new benchmarking. In *Thirty-seventh Conference on Neural Information Processing Systems Datasets and Benchmarks Track*, 2023. URL https://openreview.net/forum?id=YdjWXrdOTh.

[25] Liang, J., Pu, C., Shu, X., Xia, Y., and Xia, C. Line graph neural networks for link weight prediction. *Physica A: Statistical Mechanics and its Applications*, pp. 130406, 2025.

[26] Lichter, M., Raßmann, S., and Schweitzer, P. Computational complexity of the weisfeiler-leman dimension. In *33rd EACSL Annual Conference on Computer Science Logic (CSL 2025)*, pp. 13–1. Schloss Dagstuhl–Leibniz-Zentrum für Informatik, 2025.

[27] Lü, L. and Zhou, T. Link prediction in complex networks: A survey. *Physica A: statistical mechanics and its applications*, 390(6):1150–1170, 2011.

[28] McKay, B. D. and Piperno, A. Practical graph isomorphism, II. *Journal of Symbolic Computation*, 60:94–112, 2014.

[29] Michel, G., Nikolentzos, G., Lutzeyer, J. F., and Vazirgiannis, M. Path neural networks: Expressive and accurate graph neural networks. In *International Conference on Machine Learning*, pp. 24737–24755. PMLR, 2023.

[30] Morris, C., Ritzert, M., Fey, M., Hamilton, W. L., Lenssen, J. E., Rattan, G., and Grohe, M. Weisfeiler and leman go neural: Higher-order graph neural networks. In *Proceedings of the AAAI conference on artificial intelligence*, volume 33, pp. 4602–4609, 2019.

[31] Nickel, M., Murphy, K., Tresp, V., and Gabrilovich, E. A review of relational machine learning for knowledge graphs. *Proceedings of the IEEE*, 104(1):11–33, 2015.

[32] Rossi, A., Barbosa, D., Firmani, D., Matinata, A., and Merialdo, P. Knowledge graph embedding for link prediction: A comparative analysis. *ACM Transactions on Knowledge Discovery from Data (TKDD)*, 15(2):1–49, 2021.

[33] Shomer, H., Ma, Y., Mao, H., Li, J., Wu, B., and Tang, J. Lpformer: an adaptive graph transformer for link prediction. In *Proceedings of the 30th ACM SIGKDD Conference on Knowledge Discovery and Data Mining*, pp. 2686–2698, 2024.

[34] Sommer, C. Shortest-path queries in static networks. *ACM Computing Surveys (CSUR)*, 46(4): 1–31, 2014.

[35] Srinivasan, B. and Ribeiro, B. On the equivalence between positional node embeddings and structural graph representations. *arXiv preprint arXiv:1910.00452*, 2019.

[36] Tola, A., Myrick, J., and Coskunuzer, B. PROXI: Challenging the GNNs for link prediction. *Transactions on Machine Learning Research*, 2025. ISSN 2835-8856. URL https://openreview.net/forum?id=u9EHndbiVw.

[37] Vaswani, A., Shazeer, N., Parmar, N., Uszkoreit, J., Jones, L., Gomez, A. N., Kaiser, Ł., and Polosukhin, I. Attention is all you need. *Advances in neural information processing systems*, 30, 2017.

[38] Veličković, P., Cucurull, G., Casanova, A., Romero, A., Liò, P., and Bengio, Y. Graph attention networks. In *International Conference on Learning Representations*, 2018. URL https://openreview.net/forum?id=rJXMpikCZ.

[39] Veličković, P., Cucurull, G., Casanova, A., Romero, A., Liò, P., and Bengio, Y. Graph attention networks. In *International Conference on Learning Representations*, 2018. URL https://openreview.net/forum?id=rJXMpikCZ.

[40] Wang, H., Yin, H., Zhang, M., and Li, P. Equivariant and stable positional encoding for more powerful graph neural networks. In *International Conference on Learning Representations*, 2022. URL https://openreview.net/forum?id=e95i1IHcWj.

[41] Wang, X., Lyu, D., Li, M., Xia, Y., Yang, Q., Wang, X., Wang, X., Cui, P., Yang, Y., Sun, B., et al. Apan: Asynchronous propagation attention network for real-time temporal graph embedding. In *Proceedings of the 2021 international conference on management of data*, pp. 2628–2638, 2021.

[42] Wang, X., Yang, H., and Zhang, M. Neural common neighbor with completion for link prediction. In *The Twelfth International Conference on Learning Representations*, 2024. URL https://openreview.net/forum?id=sNFLN3itAd.

[43] Xu, K., Hu, W., Leskovec, J., and Jegelka, S. How powerful are graph neural networks?, 2019.

[44] Yang, Z., Cohen, W., and Salakhudinov, R. Revisiting semi-supervised learning with graph embeddings. In *International conference on machine learning*, pp. 40–48. PMLR, 2016.

[45] Ying, C., Cai, T., Luo, S., Zheng, S., Ke, G., He, D., Shen, Y., and Liu, T.-Y. Do transformers really perform badly for graph representation? *Advances in neural information processing systems*, 34:28877–28888, 2021.

[46] Ying, R., He, R., Chen, K., Eksombatchai, P., Hamilton, W. L., and Leskovec, J. Graph convolutional neural networks for web-scale recommender systems. In *Proceedings of the 24th ACM SIGKDD international conference on knowledge discovery & data mining*, pp. 974–983, 2018.

[47] Yun, S., Kim, S., Lee, J., Kang, J., and Kim, H. J. Neo-gnns: Neighborhood overlap-aware graph neural networks for link prediction. *Advances in Neural Information Processing Systems*, 34:13683–13694, 2021.

[48] Zhang, M. and Chen, Y. Link prediction based on graph neural networks. *Advances in neural information processing systems*, 31, 2018.

[49] Zhang, M., Li, P., Xia, Y., Wang, K., and Jin, L. Labeling trick: A theory of using graph neural networks for multi-node representation learning. *Advances in Neural Information Processing Systems*, 34:9061–9073, 2021.

[50] Zhao, Q., Ren, W., Li, T., Liu, H., He, X., and Xu, X. GraphGPT: Generative pre-trained graph eulerian transformer. In *Forty-second International Conference on Machine Learning*, 2025. URL https://openreview.net/forum?id=4RdzeucFmW.

[51] Zhou, T. Progresses and challenges in link prediction. *Iscience*, 24(11), 2021.

[52] Zhu, Z., Zhang, Z., Xhonneux, L.-P., and Tang, J. Neural bellman-ford networks: A general graph neural network framework for link prediction. *Advances in neural information processing systems*, 34:29476–29490, 2021.

A Proofs

Proposition 4.4 SP4LP does not suffer from the automorphic node problem.

Proof. According to Proposition 2.9, a model class M suffers from the *automorphic node problem* if, for every graph $G = (V, E, \mathbf{X}^0)$ and every pair of non-automorphic links (u, v) and (u', v') with $u \simeq u'$ and $v \simeq v'$, all $F \in M$ satisfy

$$F((u, v), G) = F((u', v'), G).$$

To show that SP4LP does not suffer from this problem, it suffices to exhibit one such graph and pair of links, and one instantiation $F \in$ SP4LP, for which

$$F((u, v), G) \neq F((u', v'), G).$$

Such an example is provided in Figure 1: the shortest path from v to u' consists of v, an orange node, and u', whereas the shortest path from v to u includes v, an orange node, a yellow node, another orange node, and finally u. Thus, simply using a summation as function ϕ, leads to distinct representations for links (v, u) and (v, u'). □

Theorem 4.5 SP4LP is strictly more expressive than pure GNN link representation models, NCN, the set-based horizontal GDGNN link encoder, and the degree-free vertical GDGNN link encoder. Moreover, neither Neo-GNN nor BUDDY is more expressive than SP4LP.

Proof. We proceed by prove each comparison separately.

- SP4LP is strictly more expressive than Pure GNN.

  We prove this by noting that SP4LP architecture (Equation 7) generalizes that of pure GNNs, meaning that SP4LP can simulate any pure GNN by simply ignoring the shortest path information. Thus, for any pair of non-automorphic links that a specific pure GNN can distinguish, there exists a configuration of SP4LP that distinguishes them as well. We can conclude that SP4LP is strictly more expressive than pure GNNs considering as example of pair of links indistinguishable by GNNs but distinguishable by SP4LP the one provided in the proof of Proposition 4.4.

- SP4LP is strictly more expressive than NCN.

  We first establish that SP4LP can reproduce NCN in the target-link-removed setting. Let H denote the graph used by both models for message passing and structural feature extraction, with the queried edge removed if present. Write $\mathbf{h}_w = \text{GNN}(w, H)$.

  If u and v have common neighbors in H, their shortest paths have length two and are precisely the paths (u, w, v) with $w \in N_H(u) \cap N_H(v)$. Choose ϕ to return $\mathbf{h}_w/2$ for each such three-node sequence and zero for sequences of any other length, including the disconnected-pair fallback. With summation as AGG, this yields

  $$\sum_{w \in N_H(u) \cap N_H(v)} \mathbf{h}_w.$$

  The factor $1/2$ accounts for the two orientations of each path included in $\mathcal{P}^*_H\{u, v\}$. When there are no common neighbors, the aggregate is zero, as in NCN. Choosing ρ to reproduce NCN's combination of endpoint embeddings and the common-neighbor aggregate therefore recovers its link representation. This establishes NCN $\preceq$ SP4LP under the stated setting.

  To establish strictness, consider the eight-node cycle with constant node features shown in Figure 4, with $d_H(u, v) = 3$ and $d_H(u, v') = 4$. The cycle is vertex-transitive, so all nodes receive the same embedding from a message-passing GNN. Neither queried pair has common neighbors; consequently, NCN assigns the same representation to (u, v) and (u, v'). The two links are not automorphic, since automorphisms preserve shortest-path distances. In contrast, their shortest-path sequences contain four and five nodes, respectively. Choose a nonzero constant node embedding $\mathbf{x}$, let ϕ sum the embeddings within each path, and let AGG average the resulting path representations. The two path representations are then $4\mathbf{x}$ and $5\mathbf{x}$, which a suitable ρ distinguishes. Together with the inclusion established above, this proves strictness in the target-link-removed setting.

- Neo-GNN and BUDDY do not dominate SP4LP.

  Theorem 2 of Wang et al. [42] establishes that neither Neo-GNN nor BUDDY is more expressive than NCN. Since $\mathrm{NCN} \preceq$ SP4LP, if either model M could subsume SP4LP, transitivity would imply

  $$\mathrm{NCN} \preceq \text{SP4LP} \preceq M,$$

  contradicting that result. Therefore, neither Neo-GNN nor BUDDY is more expressive than SP4LP. This does not establish that SP4LP is strictly more expressive than either model.

- SP4LP is strictly more expressive than GDGNN.

  (Horizontal GDGNN). We show that SP4LP is strictly more expressive than the set-based horizontal GDGNN link encoder. First, SP4LP subsumes horizontal GDGNN: choose the SP4LP path encoder ϕ to be permutation-invariant over the nodes on a shortest path (i.e., $\phi(\mathbf{h}_P) = \mathrm{POOL}(\{\mathbf{h}_x : x \in P\})$), and choose AGG to return the representation of the same deterministically selected shortest path $\pi(u, v)$ used by horizontal GDGNN (e.g., the path returned by a fixed shortest-path routine with a fixed tie-breaking rule). With the same decoder, the resulting SP4LP equals the horizontal GDGNN on every link query. To prove strictness, consider two non-automorphic links (u, v) and (u', v') each having a *unique* shortest path, $P = (u, a, b, v)$ and $P' = (u', b, a, v')$, with embeddings satisfying $\mathbf{h}_u = \mathbf{h}_{u'}$, $\mathbf{h}_v = \mathbf{h}_{v'}$, and $\mathbf{h}_a \neq \mathbf{h}_b$ (e.g., due to distinct node features). Any set-based horizontal GDGNN aggregates over the multiset $\{\mathbf{h}_u, \mathbf{h}_a, \mathbf{h}_b, \mathbf{h}_v\}$ and hence produces identical pooled features for P and P'; with matching endpoints, it outputs identical link representations and cannot distinguish the two queries. In contrast, SP4LP can choose an order-sensitive sequence encoder ϕ (e.g., an RNN/Transformer) such that $\phi(\mathbf{h}_u, \mathbf{h}_a, \mathbf{h}_b, \mathbf{h}_v) \neq \phi(\mathbf{h}_{u'}, \mathbf{h}_b, \mathbf{h}_a, \mathbf{h}_{v'})$, and since each query has a unique shortest path, AGG is trivial. Thus SP4LP distinguishes a pair of non-automorphic link queries that horizontal GDGNN cannot, proving strictness.

  (Vertical GDGNN). We show that SP4LP is strictly more expressive than the vertical GDGNN link encoder. For subsumption, define the SP4LP path encoder ϕ to extract only the first and last internal nodes of a shortest path: for $P = (u, x_1, \ldots, x_{\ell-1}, v)$ let $\phi(\mathbf{h}_P) = [\mathbf{h}_{x_1}; \mathbf{h}_{x_{\ell-1}}]$, and let AGG pool these two positions across all shortest paths (with the same permutation-invariant POOL as vertical GDGNN), yielding exactly the pooled feature over the vertical endpoint-neighbor set $S^{\mathrm{V}}(u, v) = (N(u) \cap W(u, v)) \cup (N(v) \cap W(u, v))$, where $W(u, v) = \{w : d(u, w) + d(w, v) = d(u, v)\}$. Using the same decoder ρ, SP4LP matches the degree-free vertical GDGNN on every link query. For strictness, consider two non-automorphic link queries (u, v) and (u', v') with unique shortest paths $P = (u, a, x, b, v)$ and $P' = (u', a, y, b, v')$, where the first/last internal nodes coincide (a and b) but the middle internal node differs ($x \neq y$), and assume $\mathbf{h}_u = \mathbf{h}_{u'}$, $\mathbf{h}_v = \mathbf{h}_{v'}$, and $\mathbf{h}_x \neq \mathbf{h}_y$ (e.g., via distinct features). Since each query has a unique shortest path, the degree-free vertical GDGNN uses the same vertical set $S^{\mathrm{V}}(u, v) = \{a, b\} = S^{\mathrm{V}}(u', v')$, hence produces identical pooled features and cannot distinguish the two queries. In contrast, SP4LP may use an order-sensitive ϕ on the full path sequence, so that $\phi(\mathbf{h}_u, \mathbf{h}_a, \mathbf{h}_x, \mathbf{h}_b, \mathbf{h}_v) \neq \phi(\mathbf{h}_{u'}, \mathbf{h}_a, \mathbf{h}_y, \mathbf{h}_b, \mathbf{h}_{v'})$ whenever $\mathbf{h}_x \neq \mathbf{h}_y$, and AGG is trivial under uniqueness of the shortest path. Therefore, SP4LP distinguishes a pair of non-automorphic link queries that the degree-free vertical GDGNN cannot, proving strictness.

  Remark (Scope). The strictness result applies to the *degree-free* vertical GDGNN class. If the vertical model is augmented with additional induced-subgraph structural features (e.g., degree-in-induced-subgraph), the inclusion and strictness relationships may change and require a separate analysis.

□

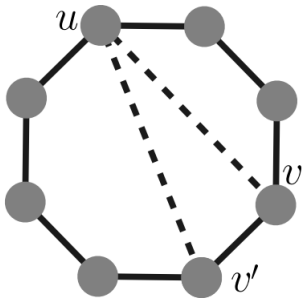

Figure 4: An eight-node cycle with constant node features. Dashed lines indicate queried pairs, not graph edges. Both (u, v) and (u, v') have no common neighbors, but their shortest-path distances are three and four, respectively. NCN assigns them identical representations, whereas a length-sensitive instantiation of SP4LP distinguishes them.

B Additional results

We complement the main results of Section 5 with additional tables reporting the standard deviation computed over five different random seeds, to better assess the stability of each method.

Real-world Datasets: Results with Standard Deviations Table 3 and Table 4 expand the main results in Table 1 by including both the mean and standard deviation of MRR and Hits@K across runs.

	Models	Cora MRR	Citeseer MRR	Pubmed MRR	Ogbl-ddi MRR	Ogbl-collab MRR	Ogbl-ppa MRR	Ogbl-Citation2 MRR
GNN	GCN	16.61 (± 0.30)	21.09 (± 0.88)	7.13 (± 0.27)	**13.46** (± 0.34)	6.09 (± 0.38)	26.94 (± 0.48)	19.98 (± 0.35)
	GAT	13.84 (± 0.68)	19.58 (± 0.84)	4.95 (± 0.14)	12.92 (± 0.39)	4.18 (± 0.33)	OOM	OOM
	SAGE	14.74 (± 0.69)	21.09 (± 1.15)	**9.40** (± 0.70)	12.60 (± 0.72)	5.53 (± 0.50)	27.27 (± 0.30)	22.05 (± 0.12)
	GAE	**18.32** (± 0.41)	25.25 (± 0.82)	5.27 (± 0.25)	3.49 (± 1.73)	OOM	OOM	OOM
GT	LPFORMER	**16.80** (± 0.52)	**26.34** (± 0.67)	**9.99** (± 0.52)	13.20 (± 0.54)	**7.62** (± 0.26)	**40.25** (± 0.24)	**24.70** (± 0.55)
	GraphGPT	8.07 (± 2.98)	8.72 (± 3.21)	3.18 (± 3.45)	>24h	1.73 (± 3.91)	>24h	>24h
SF GNN	GDGNN	6.32 (± 0.17)	7.93 (± 0.45)	0.96 (± 0.02)	>24h	>24h	>24h	>24h
	SEAL	10.67 (± 3.46)	13.16 (± 1.66)	5.88 (± 0.53)	9.99 (± 0.90)	6.43 (± 0.32)	29.71 (± 0.71)	20.60 (± 1.28)
	BUDDY	13.71 (± 0.59)	22.84 (± 0.36)	7.56 (± 0.18)	12.43 (± 0.50)	5.67 (± 0.36)	27.70 (± 0.33)	19.17 (± 0.10)
	Neo-GNN	13.95 (± 0.39)	17.34 (± 0.84)	7.74 (± 0.30)	10.86 (± 2.16)	5.23 (± 0.90)	21.68 (± 1.14)	16.12 (± 0.25)
	NCN	14.66 (± 0.95)	**28.65** (± 1.21)	5.84 (± 0.22)	12.86 (± 0.78)	5.09 (± 0.38)	35.06 (± 0.26)	**23.35** (± 0.28)
	NCNC	14.98 (± 1.00)	24.10 (± 0.65)	8.58 (± 0.59)	>24h	4.73 (± 0.86)	33.52 (± 0.26)	19.61 (± 0.54)
	NBFNet	13.56 (± 0.58)	14.29 (± 0.80)	>24h	>24h	OOM	OOM	OOM
	PEG	15.73 (± 0.39)	21.01 (± 0.77)	4.40 (± 0.41)	12.05 (± 1.14)	4.83 (± 0.21)	OOM	OOM
	MPLP	12.57 (± 0.23)	12.55 (± 0.17)	5.19 (± 0.09)	**13.94** (± 0.96)	**6.79** (± 1.02)	**41.40** (± 0.65)	23.11 (± 1.76)
	SP4LP	**28.84** (± 5.45)	**29.48** (± 10.17)	**10.87** (± 0.31)	**15.00** (± 0.57)	**9.46** (± 0.55)	**36.45** (± 1.21)	**24.91** (± 0.41)

Table 3: MRR results across all datasets, following the HeaRT evaluation setting [24]. The top three results for each metric are highlighted using **first**, **second**, and **third**. *OOM* indicates that the model ran out of memory, while *>24h* denotes that the method did not complete within 24 hours. Methods are grouped into pure GNN baselines (**GNN**), GNNs augmented with structural features (**SF GNN**), and graph transformers (**GT**).

Ablation Study: Results with Standard Deviations Similarly, Table 5 complements the ablation results in Table 2 by reporting mean and standard deviation for Cora, Citeseer, and Pubmed.

Truncated BFS. We evaluate the trade-off between predictive performance and preprocessing cost on Pubmed by limiting BFS to a maximum number of hops. Pairs reachable within the cutoff retain their exact shortest path; otherwise, we use the endpoint-only fallback (u, v). Table 6 reports results from a single run. Increasing the cutoff improves predictive performance at the cost of longer preprocessing.

Graph symmetries and empirical gains. We quantify structural graph symmetries using $r'_G = 1 - (|\mathcal{O}_G| - 1)/(|V_G| - 1)$, where $\mathcal{O}_G$ is the set of node-automorphism orbits. We compute exact

	Models	Cora Hits@10	Citeseer Hits@10	Pubmed Hits@10	Ogbl-ddi Hits@20	Ogbl-collab Hits@20	Ogbl-ppa Hits@20	Ogbl-Citation2 Hits@20
GNN	GCN	36.26 (± 1.14)	47.23 (± 1.88)	15.22 (± 0.57)	64.76 (± 1.45)	**22.48** (± 0.81)	68.38 (± 0.73)	51.72 (± 0.46)
	GAT	32.89 (± 1.27)	45.30 (± 1.30)	9.99 (± 0.64)	**66.83** (± 2.23)	18.30 (± 1.42)	OOM	OOM
	SAGE	34.65 (± 1.47)	48.75 (± 1.85)	**20.54** (± 1.40)	**67.19** (± 1.18)	21.26 (± 1.32)	69.49 (± 0.43)	53.13 (± 0.15)
	GAE	**37.95** (± 1.24)	49.65 (± 1.48)	10.50 (± 0.46)	17.81 (± 9.80)	OOM	OOM	OOM
GT	LPFORMER	34.03 (± 1.33)	**51.72** (± 1.83)	**21.43** (± 1.30)	62.66 (± 0.37)	21.04 (± 0.16)	**84.10** (± 0.10)	**57.30** (± 0.50)
	GraphGPT	18.03 (± 2.12)	19.78 (± 1.11)	5.98 (± 3.21)	>24h	6.24 (± 2.67)	>24h	>24h
SF GNN	GDGNN	15.97 (± 0.31)	14.25 (± 1.15)	1.10 (± 0.02)	>24h	>24h	>24h	>24h
	SEAL	24.27 (± 6.74)	27.37 (± 3.20)	12.47 (± 1.23)	49.74 (± 2.39)	21.57 (± 0.38)	76.77 (± 0.94)	48.62 (± 1.93)
	BUDDY	30.40 (± 1.18)	48.35 (± 1.18)	16.78 (± 0.53)	58.71 (± 1.63)	**23.35** (± 0.73)	71.50 (± 0.68)	47.81 (± 0.37)
	Neo-GNN	31.27 (± 0.72)	41.74 (± 1.18)	17.88 (± 0.71)	51.94 (± 10.33)	21.03 (± 3.39)	64.81 (± 2.26)	43.17 (± 0.53)
	NCN	35.14 (± 1.04)	**53.41** (± 1.46)	13.22 (± 0.56)	**65.82** (± 2.66)	20.84 (± 1.31)	81.89 (± 0.31)	53.76 (± 0.20)
	NCNC	**36.70** (± 1.57)	**53.72** (± 0.97)	18.81 (± 1.16)	>24h	20.49 (± 3.97)	**82.24** (± 0.40)	51.69 (± 1.48)
	NBFNet	31.12 (± 0.75)	31.39 (± 1.34)	>24h	>24h	OOM	OOM	OOM
	PEG	36.03 (± 0.75)	45.56 (± 1.38)	8.70 (± 1.26)	50.12 (± 6.55)	18.29 (± 1.06)	OOM	OOM
	MPLP	27.70 (± 1.51)	27.33 (± 3.00)	10.97 (± 0.31)	59.17 (± 1.65)	**25.10** (± 1.01)	**84.80** (± 0.98)	**55.51** (± 1.12)
	SP4LP	**45.39** (± 9.58)	49.52 (± 9.77)	**23.01** (± 0.39)	47.96 (± 3.82)	20.00 (± 1.20)	76.9 (± 1.11)	**55.45** (± 0.92)

Table 4: Hits@K (%) results across all datasets, following the HeaRT evaluation setting [24]. The top three results for each metric are highlighted using **first**, **second**, and **third**. *OOM* indicates that the model ran out of memory, while *>24h* denotes that the method did not complete within 24 hours. Methods are grouped into pure GNN baselines (**GNN**), GNNs augmented with structural features (**SF GNN**), and graph transformers (**GT**).

Models	**Cora**		**Citeseer**		**Pubmed**	
	MRR	Hits@10	MRR	Hits@10	MRR	Hits@10
GNN + SP len.	8.32 (± 0.28)	20.02 (± 0.67)	21.13 (± 0.99)	45.05 (± 1.24)	8.52 (± 0.01)	15.32 (± 0.66)
Sequence Model	16.86 (± 1.26)	36.03 (± 1.75)	10.93 (± 2.93)	19.23 (± 4.20)	7.12 (± 0.75)	13.56 (± 0.85)
SP4LP	**28.84** (± 5.45)	**45.39** (± 9.58)	**29.48** (± 10.17)	**49.52** (± 9.77)	**10.87** (± 0.31)	**23.01** (± 0.39)

Table 5: Ablation study results (%). MRR and Hits@K with mean and std. deviations over 5 runs with different seeds.

orbits using nauty [28] on the three citation datasets, for which this computation was feasible. Table 7 compares this measure with the MRR improvement over GCN. We observe no monotonic relationship between graph symmetry and the improvement of SP4LP. Thus, automorphisms motivate pair-specific representations, but do not alone explain empirical gains, which also depend on node features, path distributions, optimization, and architectural inductive biases.

C Datasets statistics

Table 8 summarizes the main datasets used in our link prediction experiments. Cora, Citeseer, and Pubmed are well-known citation networks frequently used as benchmarks for graph-based learning methods. These datasets are relatively small, both in the number of nodes and edges. In contrast, the datasets from the Open Graph Benchmark (OGB), namely ogbl-collab and ogb-ddi, are substantially larger and more complex, offering challenging scenarios for evaluating model scalability and performance on large-scale graphs.

For all datasets, we adopt the splits provided by the [24] setting.

Shortest-path statistics. Table 9 reports shortest-path statistics for each dataset and split, separately for positive and negative queries. No-path percentages are computed over all queries in the corresponding group; means and variances are computed only over pairs connected by a finite path. Disconnected pairs use the endpoint-only fallback described in Section 4. Such pairs are particularly frequent in the smaller citation graphs, while their prevalence is generally low in the validation and test splits of the larger benchmarks. Statistics use undirected, unweighted graphs. Validation/test queries use the training-only graph. For the three citation datasets, training statistics use a `train_val` subset sampled with seed 999 and matched to the validation size; each queried positive edge is removed before evaluating it and its associated negatives. For OGB training statistics, 70% of shuffled training-edge occurrences form the message-passing graph and the remaining 30%

Maximum hops	MRR (%)	Hits@10 (%)	Preprocessing (s)
2	7.00	14.98	1
5	7.59	16.34	150
7	9.16	18.21	320
Full	10.87	23.01	570

Table 6: Predictive performance and shortest-path preprocessing time for truncated BFS on Pubmed. Full denotes BFS without a depth cutoff. Results are from a single run.

Dataset	r'_G	GCN MRR	SP4LP MRR	Δ MRR
Cora	0.127	16.61	28.84	+12.23
Citeseer	0.372	21.09	29.48	+8.39
Pubmed	0.341	7.13	10.87	+3.74

Table 7: Structural graph symmetries and MRR gains over GCN. MRR is reported in percent and gains in percentage points.

provide positive queries. Repeated pairs can occur in both subsets, yielding distance-one positive queries.

D Experimental Settings

This section outlines the experimental setup used to evaluate all models. We describe the computational resources and the hyperparameter search space. Moreover for SP4LP we include details regarding how the calculation of the shortest path is performed. Details are reported below.

Computational Resources All experiments were conducted on a workstation running Ubuntu 22.04 with an AMD Ryzen 9 7950X CPU (32 threads), 124GB of RAM, and two NVIDIA GeForce RTX 4090 GPUs (24GB each).

Hyperparameters All models are tuned using a grid search over learning rate $\in [1 \times 10^{-2}, 1 \times 10^{-3}]$, dropout $\in [0, 0.7]$, weight decay $\in [0, 10^{-4}, 10^{-7}]$, number of GNN layers $\in \{1, 2, 3\}$, hidden dimensions $\in \{32, 64, 128, 256\}$ and prediction layers $\in \{1, 2, 3\}$. For large-scale datasets, we follow the reduced search space adopted in Li et al. [24] to avoid excessive compute. For SP4LP, we additionally explore the choice of GNN component $\in \{\text{GCN}, \text{GraphSAGE}, \text{GAT}\}$ and sequence model $\in \{\text{LSTM}, \text{Transformer}\}$, the best models are shown in Table 10. The best hyperparameters are selected based on validation performance. All reported metrics are averaged over 5 different seeds.

Shortest path calculation for SP4LP To compute shortest paths for SP4LP, we use the `networkx.shortest_path` BFS implementation [14]. Importantly, we compute and cache shortest paths only for the train/validation/test links provided by the HeaRT benchmark splits. During training, message passing and shortest-path extraction use a subset of training edges disjoint from the supervised positive edges. For validation and testing, both use the training-only graph, without adding validation or test edges. A single BFS can serve multiple queries sharing the same source node, provided that they use the same path-extraction graph. Queries evaluated on different edge-masked graphs require separate computations. The preprocessing cost is amortized through caching. Table 6 reports the trade-off between preprocessing time and predictive performance on Pubmed. The cached paths are reused across all training epochs and inference batches. No all-pairs shortest path computation is performed. When multiple shortest paths exist, we select the first path returned by BFS under a fixed adjacency ordering and cache it, keeping the selection deterministic throughout training and evaluation. To assess sensitivity to this choice, we fixed a trained GCN–Transformer model on Cora and varied only the paths used at test time. For each test link, we sampled up to ten alternative shortest paths, using repetition when fewer alternatives were available. Across these path selections, the standard deviations were 0.10 percentage points for MRR and 0.01 percentage points for Hits@10, indicating low sensitivity in this experiment.

Dataset	Cora	Citeseer	Pubmed	ogbl-collab	ogbl-ddi	ogbl-ppa	ogbl-citation2
#Nodes	2708	3327	18717	235868	4267	576289	2927963
#Edges	5278	4676	44327	1285465	1334889	30326273	30561187

Table 8: Dataset statistics.

In our implementation of SP4LP, the sequential encoder can be instantiated as a Transformer with learnable positional encodings. We use PyTorch's TransformerEncoder, composed of TransformerEncoderLayer blocks with 4-head self-attention, feedforward sublayers, ReLU activation, and dropout. We tune the number of layers $\in \{1, 2\}$, attention heads $\in \{2, 3, 4\}$, and feedforward dimensionality $\in \{32, 64, 128\}$. A trainable positional embedding matrix is added to node embeddings to preserve path order. Variable-length paths are handled via a source key padding mask, and the output is aggregated using masked mean pooling followed by layer normalization. The resulting path representation is then combined with the GNN-derived embeddings of the source and target nodes to compute the final link score.

For the LSTM-based encoder, we implement both unidirectional and bidirectional variants using PyTorch's nn.LSTM. Input sequences are packed with pack_padded_sequence to handle variable-length paths. We tune the number of layers $\in \{1, 2\}$ and hidden size $\in \{32, 64, 128\}$. The final hidden state (or the concatenation of forward and backward states in the bidirectional case) is used as the path representation and combined with the GNN-based node embeddings for link prediction. Node embeddings are obtained via a GNN encoder selected from GCN, GAT, or GraphSAGE, depending on the experimental setting.

Reproducibility details. The precomputed `gnn_feature` and `entity_embedding` files used by the small-dataset pipeline come from the HeaRT data release and are loaded using the same procedure as its baselines. Training negatives follow the HeaRT baseline sampling procedure (`torch.randint`), without explicitly excluding held-out positive edges. Consequently, sampled training negatives may overlap with held-out positives. For every SP4LP run reported in Table 1, all training, validation, and test paths, including paths for sampled training negatives, were recomputed from scratch with `-force_recompute_paths`, bypassing existing caches.

E Computational Complexity

In this section, we analyze the computational complexity of our proposed SP4LP model for link prediction, following the formalism and notation introduced in [42]. This framework allows a direct comparison with prior approaches such as GAE, Neo-GNN, BUDDY, PEG, SEAL, NCN, and NCNC.

Let n be the number of nodes, m the number of edges, Δ the maximum degree, d the dimensionality of node features or embeddings, t the number of target links to predict, and k the length of the shortest path between node pairs (typically $k \ll n$). We express total time complexity as $\mathcal{O}(B + C \cdot t)$, where B is the precomputation cost (independent of t), and C is the per-link cost.

Our SP4LP method follows the GNN-then-Structural-Feature (SF) paradigm [42], applying a Message Passing Neural Network once across the entire graph to compute node embeddings, then leveraging shortest path extraction combined with sequence modeling for each candidate link.

Following the paradigm, the precomputation cost of SP4LP is:

$$B = \mathcal{O}(n\Delta d + nd^2 + T_{\text{sp}})$$

where: $n\Delta d$ accounts for neighborhood aggregation in the GNN, nd^2 represents linear transformations in GNN layers, T_{sp} is the cost of computing shortest paths (e.g., via BFS).

For sparse graphs, single-source BFS runs in $O(m)$ time. Although all-pairs shortest paths (APSP) would cost $O(nm)$, SP4LP never computes APSP. In all benchmark settings, we compute shortest paths only for the supervised train/validation/test links. Let S be the number of distinct endpoint nodes among these links. The total preprocessing cost is therefore

$$T_{\text{sp}} = O(S \cdot m),$$

Dataset	Split	Queries	Total	No path	No path (%)	Mean	Variance
Cora	Train†	Pos.	263	35	13.31	3.00	2.13
	Train†	Neg.	131500	30077	22.87	6.87	5.14
	Val.	Pos.	263	41	15.59	3.09	2.71
	Val.	Neg.	131500	18828	14.32	5.48	5.33
	Test	Pos.	527	77	14.61	3.15	2.74
	Test	Neg.	263500	36857	13.99	5.48	5.20
Citeseer	Train†	Pos.	227	77	33.92	3.18	6.80
	Train†	Neg.	113500	78813	69.44	9.77	12.93
	Val.	Pos.	227	77	33.92	3.12	4.16
	Val.	Neg.	113500	66483	58.58	7.64	17.27
	Test	Pos.	455	163	35.82	3.13	6.31
	Test	Neg.	227500	129764	57.04	7.58	17.59
Pubmed	Train†	Pos.	2216	549	24.77	3.10	1.89
	Train†	Neg.	1108000	175019	15.80	6.62	2.47
	Val.	Pos.	2216	512	23.10	3.05	1.63
	Val.	Neg.	1108000	171651	15.49	4.34	5.38
	Test	Pos.	4432	1091	24.62	3.04	1.51
	Test	Neg.	2216000	364645	16.46	4.53	5.53
ogbl-ddi	Train	Pos.	320374	30	0.00936	2.00	0.00228
	Train	Neg.	320374	3759	1.17	2.31	0.25
	Val.	Pos.	1000	0	0	2.00	0
	Val.	Neg.	500000	0	0	2.00010	0.000100
	Test	Pos.	1000	0	0	2.00	0
	Test	Neg.	500000	0	0	2.00019	0.000190
ogbl-collab	Train	Pos.	353716	18239	5.16	1.81	0.42
	Train	Neg.	353716	48568	13.73	7.30	3.07
	Val.	Pos.	60084	1111	1.85	2.17	2.10
	Val.	Neg.	30042000	531855	1.77	3.08	4.53
	Test	Pos.	46329	944	2.04	2.50	2.39
	Test	Neg.	23164500	420641	1.82	3.05	4.06
ogbl-ppa	Train	Pos.	6369580	4652	0.0730	2.11	0.12
	Train	Neg.	6369580	82591	1.30	4.39	0.63
	Val.	Pos.	100000	0	0	2.06	0.06
	Val.	Neg.	50000000	47	0.000094	3.66	0.73
	Test	Pos.	100000	4	0.004	2.06	0.06
	Test	Neg.	50000000	1057	0.002114	3.66	0.73
ogbl-citation2	Train	Pos.	9116399	97250	1.07	2.39	0.59
	Train	Neg.	9116399	514395	5.64	6.41	1.53
	Val.	Pos.	86596	69	0.0797	2.29	0.41
	Val.	Neg.	43298000	19457	0.0449	4.78	3.30
	Test	Pos.	86596	77	0.0889	2.29	0.40
	Test	Neg.	43298000	21591	0.0499	4.74	3.47

Table 9: Shortest-path statistics for the analyzed query sets. Total and No path report the number of queries and disconnected queries, respectively. Means and population variances are computed over finite shortest-path distances only; the endpoint-only fallback is excluded. Distances are measured in hops. †For Cora, Citeseer, and Pubmed, training statistics refer to the sampled `train_val` subset and its associated negative queries, rather than the full training set.

Parameter	Cora	Citeseer	Pubmed	ogbl-collab	ogbl-ddi	ogbl-ppa	ogbl-citation2
GNN	GCN	GCN	SAGE	SAGE	GCN	GCN	GCN
Learning rate	0.001	0.01	0.001	0.001	0.01	0.001	0.01
Dropout	0.5	0.5	0.1	0	0	0.3	0.3
Weight decay	0	10^{-7}	0	0	0	0	0
GNN layers	1	1	2	3	3	3	3
GNN hidden dimension	128	128	128	256	256	256	128
Predictor layers	3	2	3	3	3	3	3
Batch size	1024	1024	1024	65536	65536	65536	65536
Sequence encoder	Transformer	LSTM	Transformer	Transformer	Transformer	Transformer	Transformer
Sequence layers	2	2	2	2	2	2	2
Attention heads	4	–	4	4	4	4	4
Path hidden dimension	128	128	128	64	64	64	64
Path dropout	0.1	0.1	0.1	0.2	0.2	0.2	0.2
Predictor hidden dimension	256	256	256	64	64	64	64

Table 10: Selected hyperparameters for the reported SP4LP results. SAGE denotes GraphSAGE; attention heads are not applicable to the LSTM encoder.

typically several orders of magnitude smaller than $O(nm)$. Once these paths are cached, no BFS is performed during training or batched inference. In fully inductive scenarios, shortest-path trees for new nodes can be obtained via a single BFS per new node, which provides distances and parent pointers to all existing nodes at once. The per-link inference cost of SP4LP is thus

$$C = O(kd + T_{\text{seq}}),$$

where k is the path length and d the embedding dimension, making it independent of the graph size n. T_{seq} denotes the cost of a sequence model (e.g., LSTM, Transformer) applied to the node embeddings along that path.

Importantly, since both the GNN embeddings and shortest paths can be precomputed, B is incurred only once. Given that k is typically small in practice, C remains low even at scale. Unlike subgraph-based methods such as SEAL, which require per-link GNN inference over extracted neighborhoods, SP4LP performs lightweight sequence modeling on compact paths, supporting efficient batched inference. Additionally, the framework is flexible: T_{sp} can be cached or approximated [34], and T_{seq} depends on the chosen architecture and path length.

We summarize the complexities in the following table:

Method	**B**	**C**
GAE	$n\Delta d + nd^2$	d^2
Neo-GNN	$n\Delta d + nd^2 + n\Delta^l$	$\Delta^l + d^2$
BUDDY	$n\Delta d + nh$	$h + d^2$
SEAL	0	$\Delta^{(l+1)}d + \Delta^l d^2$
NCN	$n\Delta d + nd^2$	$\Delta d + d^2$
NCNC	$n\Delta d + nd^2$	$\Delta^2 d + \Delta d^2$
PEG	$n\Delta d + nd^2 + nD^2$	d^2
SP4LP	$n\Delta d + nd^2 + T_{\text{sp}}$	$kd + T_{\text{seq}}$

Table 11: Comparison of precomputation (B) and per-link (C) complexities across methods.

All methods conform to the form $\mathcal{O}(B + C \cdot t)$, with a one-time graph-level computation and a per-target-link cost. In the table, h is the cost of the hash function used in BUDDY, l denotes the radius of local neighborhoods in Neo-GNN and SEAL, and D denotes the number of Laplacian eigenvectors used for spectral positional encoding in PEG. GAE, NCN, and BUDDY are efficient but limited in expressiveness. NCNC enhances NCN via soft neighbor completion at a slightly higher cost. PEG incorporates spectral encoding ($\mathcal{O}(nD^2)$), while SEAL is the most computationally intensive due to subgraph extraction and per-link GNN processing. SP4LP, in contrast, strikes a balance between efficiency and expressiveness by combining GNN-based embeddings with sequence modeling over shortest paths, whose cost can be mitigated via approximation techniques [34], ensuring scalability for large graphs.